I R A M P
3(1), June 2012, pp. 1-15

ISSN: 2229-3159

Bound and Resonance States of Astrophysically Important Highly Stripped *Al* under Debye Plasma Screening

J. K. SAHA[a], S. BHATTACHARYYA[b,*], AND T. K. MUKHERJEE[a]

[a]Narula Institute of Technology, Agarpara, Kolkata-700109, India
[b]Dept. of Physics, Auburn University, AL 36849, USA, E-mail: sukhamoy.b@gmail.com
**Dept. of Physics, Acharya Prafulla Chandra College, New Barrackpore, Kolkata-700131, India*

ABSTRACT: The energy eigenvalues of doubly excited metastable bound $2pnp$ ($^3P^e$) (n = 2–8) states of highly stripped ion Al^{11+} are estimated under weakly coupled plasma screening for the first time using an explicitly correlated Hylleraas-type basis in the framework of the Rayleigh–Ritz variational principle. Resonance energies and widths of $3pnp$ ($^3P^e$) (n = 3–8) and $3dnd$ ($^3P^e$) (n = 3–7) states of Al^{11+} below N=3 ionization threshold of Al^{12+} have also been evaluated for the first time by using stabilization method. The Debye screening model has been employed to include the effect of weakly coupled plasma background.

I. INTRODUCTION

The quantum mechanical description of the doubly excited states (DES) of two-electron atoms has become a subject of extensive theoretical investigation in various disciplines like astrophysical data analysis [1], diagnosis of lines observed in solar corona [2], high temperature discharges [3] and plasma diagnostics [4]. After the pioneering experiment of Madden and Codling [5] on *DES* of helium, remarkable interest has been generated both experimentally [6-17] as well as theoretically [18-30] in studying these DES of two-electron systems including highly stripped ions. These states lie above the one-electron continuum and on the basis of stability, can be classified into two general groups, as bound and resonance states, depending on the angular momentum coupling scheme and parity conservation rule [19]. The exactly quantized DES can decay to the lower excited states through electronic dipole interaction giving rise to sharp spectral lines and the other set of states exhibit non-radiative decay. They are found to be very important in dielectronic recombination processes occurring in solar corona for maintaining its equilibrium, guided mainly by the balance between various ionization and recombination processes and in high temperature plasma diagnostics [31-33]. A large number of such states for highly stripped helium-like ions have been observed in solar flare and corona [34, 35] and also by the YOHKOH satellite observations [31, 36, 37] on the upper solar atmosphere. Strong spectral lines belonging to hydrogen and helium-like ions of aluminum, silicon, sulphur, argon etc have been reported in different astrophysical observations [38, 39]. The astrophysical data of highly stripped ions may also provide valuable diagnostics on the physical condition of the stellar wind [40].

In the present work, we have focused on studying the doubly excited ($^3P^e$) states of helium-like aluminum below N = 2 and 3 ionization thresholds of Al^{12+}. In recent high resolution astrophysical observations with satellite-borne X-ray telescopes (*Chandra*, *XMM Newton* and *Suzaku*), it has become possible to observe and study the so far weak spectral features of aluminum in various astrophysical objects. Al is apparent in the highest signal-to-noise *Chandra* grating spectra from active galaxies [41, 42], in the spectrum of the high mass X-ray binary Vela X-1 [43], in the spectra of several active stars observed by *XMM-Newton* and *Chandra* gratings [44], in the black hole candidate Cyg X-1 [45]. Spectral lines of different charge states of aluminum were detected with *XMM Newton* [46] in various clusters of galaxies. The aluminum abundance in the hot interstellar medium of the elliptical galaxy NGC 4472 has been reported from the analysis of *Suzaku* and *XMM Newton* spectra [47]. From the high-resolution

Chandra spectrum of the micro quasar GRO J1655-40, the abundances of odd-*Z* elements including aluminum have been observed from K-line absorption spectra [48]. Schulz *et al.* [49] observed the prototype Z-source Cyg X-2 twice with *Chandra* at very high spectral resolution where strong emission lines of He-like Al was reported. The coronal Al abundance of the eclipsing binary star AR Lacertae has been determined by Huenemoerder *et al.* [50] where they have used the high-resolution H- and He-like spectra of Al recorded with the *Chandra* High Energy Transmission Grating spectrograph. Moreover, spectral lines of hydrogen and helium-like Al have also been observed in different laboratory plasma experiments [53-57]. In comparison to astrophysical data and laboratory measurements, there are very few theoretical calculations [51, 52] available on helium-like Al. The radiative lifetimes of singly excited states of He-like Al in astrophysical plasma conditions were reported by Kosarev *et al.* [51] where they used density matrix formalism. In a recent work, Palmeri *et al.* [52] have reported radiative and Auger decay data and other spectral properties for different charge states of Al including Al^{11+} but they have not reported any resonance state of Al^{11+}. Under such circumstances, we have made an attempt here to estimate the energy eigenvalues of doubly excited meta-stable bound $2pnp$ ($^3P^e$) (n = 2–8) states and resonance parameters *i.e.* position and widths of $3pnp$ ($^3P^e$) (n = 3–8) and $3dnd$ ($^3P^e$) (n = 3–7) resonance states of helium-like aluminum below N=3 ionization threshold of Al^{12+} not only in free case but also in weakly coupled plasma background for the first time. It is worthwhile to mention that the spectral properties of atoms and molecules under external plasma background are greatly modified as compared to free systems due to the alteration of the effective potential felt by the charge-distribution. The plasma coupling strength Γ is defined as the ratio of average Coulomb potential energy between pairs of particles and their kinetic energy and for a weakly coupled plasma environment, the coupling parameter $\Gamma << 1$ which indicates high temperature and relatively low density of plasma components as well as the surrounding environment available in astrophysical context. In the present scenario, theoretical study of the effect of plasma on the *DES* of highly charged two-electron atoms is very limited [58, 59]. For the investigation under weakly coupled plasma, we have used the Debye model [60] where screened Coulomb or Yukawa type potential is considered to describe the particle interactions. The advantage of the Debye model [60] lies in the fact that the screening constant is a function of temperature and plasma density and thus a variety of plasma conditions can be simulated by varying the screening constant. In order to incorporate the electron-electron correlation effect, the trial wave function is expanded in multi-exponent Hylleraas-type basis set. The meta-stable bound ($^3P^e$) states have been studied within the framework of the Rayleigh–Ritz variational principle whereas the resonance parameters of the autoionizing ($^3P^e$) states have been evaluated by using stabilization method [62]. We have also calculated the energy values of hydrogen-like Al in *2p* and *3s* states in presence of Debye plasma in variational method. A brief discussion on the methodology is given in Section II followed by a discussion on the results in Section III.

II. THEORY

The modified non-relativistic Hamiltonian of two electron system in presence of an external plasma environment can be represented by

$$H = \sum_{i=1}^{2}\left[-\frac{1}{2}\nabla_i^2 + V_{eff}(r_i)\right] + V'_{eff}(r_{12}) \tag{1}$$

where, structure of the one body effective potential $V_{eff}(r_i)$ depends on the type of coupling of the plasma with the atomic charge cloud. Atomic units are used throughout. In case of weakly coupled plasma, the coulomb potential can be well approximated by screened Coulomb potential [60],

$$V_{eff}(r_i) = -Z\frac{e^{-\mu r_i}}{r_i} \tag{2}$$

where, Z is the nuclear charge and μ is the Debye screening parameter.

If the screening by both ions and electrons is envisaged, then the expression for μ [60] would be,

$$\mu = \left[\frac{4\pi\left(1 + Z_{eff}\right)n}{kT} \right]^{\frac{1}{2}} \tag{3}$$

which is a function of temperature (T) and number density (n) of the plasma electrons and the effective charge of the ions in the surrounding plasma and is given by,

$$Z_{eff} = \frac{\sum_i Z_i^2 n_i}{\sum_i Z_i n_i} \tag{4}$$

In case of fully ionized plasma comprising a single nuclear species, Z_{eff} should be replaced by Z and if we consider the screening by electron only, then we can set $Z_{eff} = 0$ in equation (3).

The two body potential for the weakly coupled plasma model is given by,

$$V'_{eff}(r_{12}) = \frac{e^{-\mu r_{12}}}{r_{12}} \tag{5}$$

The Debye screening length (D) is defined as the inverse of Debye screening parameter (μ). The smaller values of D is associated with stronger screening.

For any triplet P state of even parity arising from two p-electrons, the variational equation [62] is given by,

$$\delta \int \left[\left(\frac{\partial f_1^0}{\partial r_1} \right)^2 + \left(\frac{\partial f_1^0}{\partial r_2} \right)^2 + \left(r_1^{-2} + r_2^{-2} \right) \left(\frac{\partial f_1^0}{\partial \theta_{12}} \right)^2 + \frac{\left(r_1^{-2} + r_2^{-2} \right) \left(f_1^0 \right)^2}{\sin^2 \theta_{12}} + 2\left(V - E\right)\left(f_1^0 \right)^2 \right] dV_{r_1, r_2, \theta_{12}} = 0 \tag{6}$$

subject to the normalization condition,

$$\int \left(f_1^0 \right)^2 dV_{r_1, r_2, \theta_{12}} = 1 \tag{7}$$

The symbols in equation (6) and (7) are the same meaning as of ref. [62]. The correlated wave function is given by,

$$f_1^0(r_1, r_2, r_{12}) = \sum_{i=1}^{9} \eta_i(1)\,\eta_i(2) \left[\sum_{l>0} \sum_{m>0} \sum_{n\geq 0} C_{lmn} r_1^l r_2^m r_{12}^n \sin\theta_{12} + exchange \right] + \sum_{i=1}^{9} \sum_{\substack{j=1 \\ i \neq j}}^{9} \left[\eta_i(1)\,\eta_j(2) \sum_{l>0} \sum_{m>0} \sum_{n\geq 0} C_{lmn} r_1^l r_2^m r_{12}^n \sin\theta_{12} + exchange \right] \tag{8}$$

with

$$\eta_j(i) = e^{-\sigma_j r_i} \tag{9}$$

where σ's are the non-linear parameters. In a multi-exponent basis set, if there are p number of non-linear parameters, the number of terms in the radially correlated basis is $\frac{p(p+1)}{2}$ and therefore the dimension of the full basis (N) including angular correlation will be $\left[\frac{p(p+1)}{2} \times q \right]$, where q is the number of terms involving r_{12}. For example, as

we have used here nine non-linear parameters, the number of terms in the radially correlated basis is 45 and, with 10 terms involving different powers of r_{12}, the dimension of the full basis (N) becomes 450. The ranges of l, m, n considered here are $0 \le l \le 1$, $0 \le m \le 1$ and $0 \le n \le 8$ respectively. In the present method we have taken the nine different values of σ in a geometrical sequence: $\sigma_i = \sigma_{i-1}\,\gamma$, γ being the geometrical ratio. A discussion on the choice of specific number of non-linear parameters in the wavefunction is given by Saha *et. al.* [63]. The wavefunction can be squeezed or can be made more diffuse by changing the geometrical ratio (γ) keeping σ_1 constant throughout. To have a preliminary guess about the initial and final nonlinear parameter σ values of the sequence, we optimize the energy eigenvalue of $^3P^e$ states of Al^{11+} below $N = 2$ ionization threshold using Nelder-Mead procedure [64]. The energy eigenroots are then obtained by solving the generalized eigenvalue equation,

$$\underline{\underline{H}}\,\underline{C} = E\,\underline{\underline{S}}\,\underline{C} \tag{5}$$

where, $\underline{\underline{H}}$ is the Hamiltonian matrix, $\underline{\underline{S}}$ is the overlap matrix and E's are the energy eigenroots. For each Debye screening parameter (μ), repeated diagonalization of the Hamiltonian matrix in the Hylleraas basis set of 450 parameters is done in the present work for 400 different values of γ ranging from 0.41 a.u. to 0.77 a.u. The plot of each energy eigenroot versus γ produces the stabilization diagram. The density of resonance states is then calculated from the stabilization diagram and by fitting with a Lorentzian profile we have estimated the parameters of a particular resonance state. All calculations are carried out in quadruple precision to ensure a better numerical stability.

The energy eigenvalues of $2p$ and $3s$ states of the plasma embedded Al^{12+} have also been calculated by using Ritz variational technique considering the wavefunction as,

$$\psi = \sum_l C_l r^l \exp(-\eta r) \tag{8}$$

Where, η's are the nonlinear parameter and C's are the linear variational coefficients. For $He^+(2p)$ state we have considered 14 parameters basis set whereas for $He^+(3s)$ state we have taken 13 parameters in the basis set where l is ranging from 0 to 5.

III. RESULTS AND DISCUSSION

For Debye length $D = 50$ a.u., a portion of the stabilization diagram for $^3P^e$ states originating from two electrons of Al^{11+} having same azimuthal quantum numbers is given in figure 1. In this diagram we have plotted first 40 eigenroots of $^3P^e$ symmetry of Al^{11+} for 400 different values of γ ranging from 0.41 a.u. to 0.77 a.u. From figure 1, it is clear that there exist two classes of states:

1. Roots which are lying below $N = 2$ ionization threshold of Al^{12+}, are insensitive with the variation in γ. Thus following the analysis given by Saha *et. al.* [65], these $^3P^e$ states due to $2pnp$ configuration are metastable bound *i.e.* stable against autoionization.
2. Roots lying above $N = 2$ but below $N = 3$ ionization threshold of Al^{12+} are sensitive with the variation in γ and gives rise to flat plateau in the vicinity of avoided crossings of the energy eigenroots for some particular energy value which is a clear signature of $^3P^e$ resonance states.

The present calculated bound state energy eigenvalues ($-E$) of $2pnp$ ($^3P^e$) [$n = 2$–8] states of Al^{11+} as well as the Al^{12+} ($2p$) energies for different Debye length ranging from ∞ (Debye screening parameter $\mu = 0.0$ a.u.) corresponding to free case to 2 a.u. (Debye screening parameter $\mu = 0.5$ a.u.) are given in Table 1. The variation of eigenvalues ($-E$) of $2pnp$ ($^3P^e$) [$n = 2$–8] states of Al^{11+} as well as the Al^{12+} ($2p$) energies with Debye screening parameter (μ) is illustrated in Figure 2(a) and those with Debye length (D) is given in Figure 2(b). An increase of the Debye screening parameter (μ) or decrease in Debye length (D) gradually destabilizes the helium-like aluminum by pushing the energy levels towards continuum and ultimately ionizing it as is evident from the figure 1 as well the values quoted in Table 1. It is also evident that for higher excited states this destabilization occurs at a lower value of screening parameter.

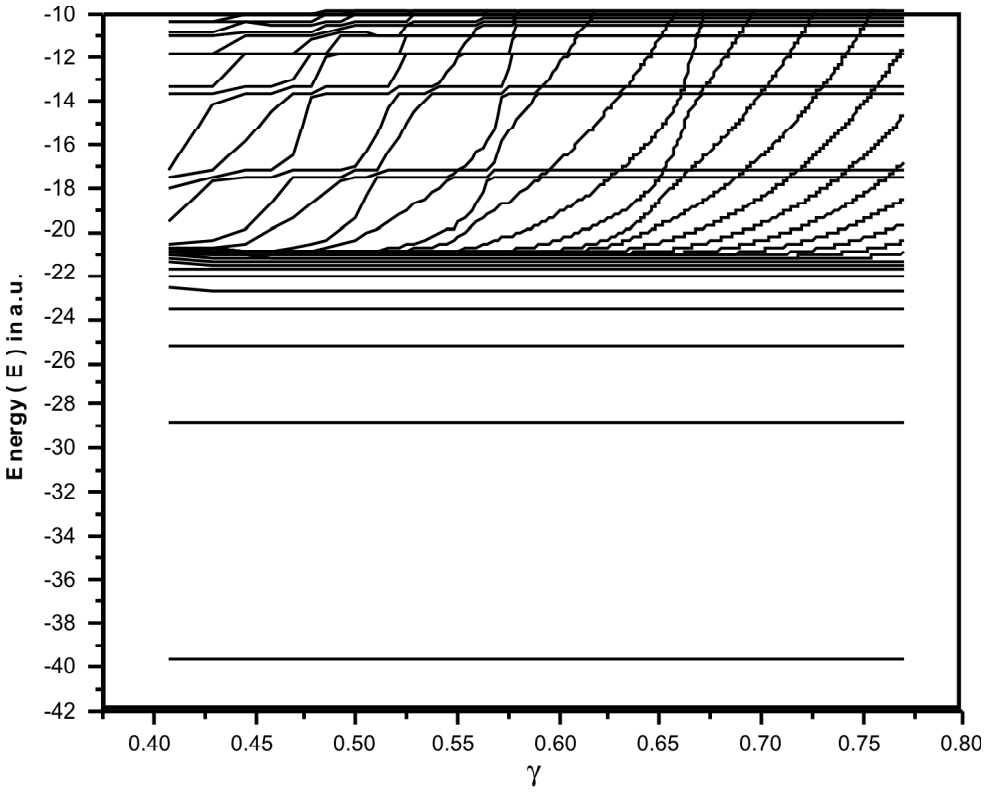

Figure 1: Stabilization diagram for $^3P^e$ states of Al^{11+} in Debye plasma of D = 50 a.u.

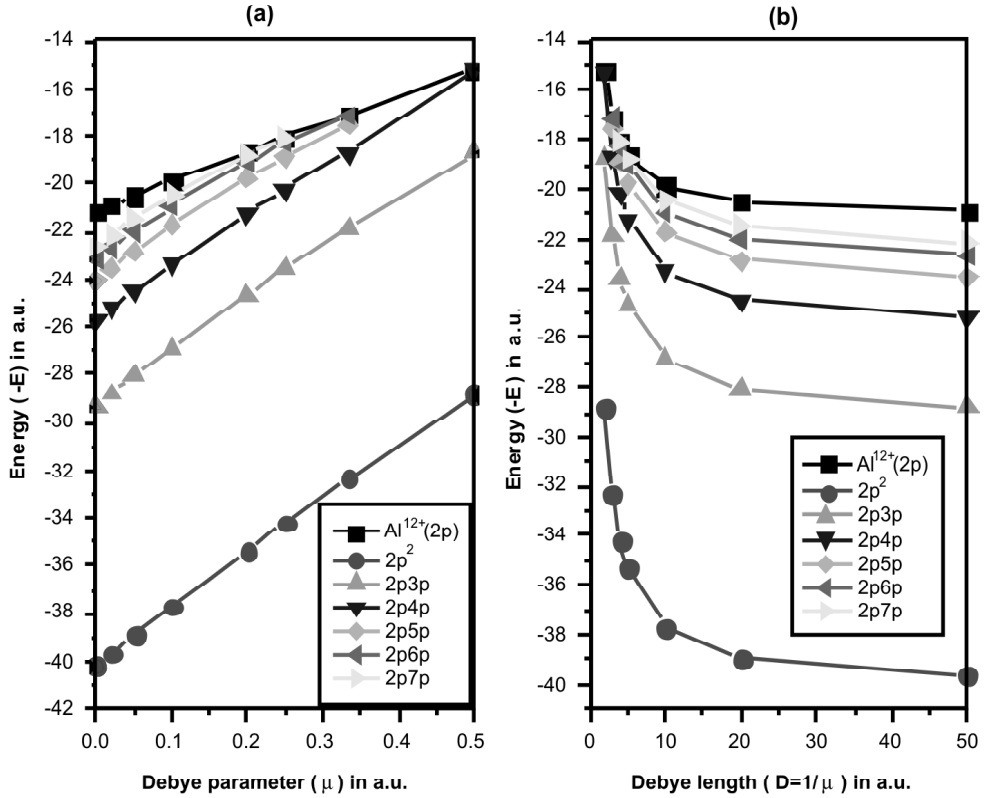

Figure 2: The variation of the bound 2*pnp* (*n*=2-7) ($^3P^e$) state energies of Al^{11+} along with Al^{12+} (2*p*) energies vs. different Debye screening parameter (μ) is given in (a) and that with Debye length (*D*) is given in (b)

Table 1
Energy Eigenvalues of Doubly Excited Metastable bound $2pnp$ ($^3P^e$) [n = 2-8] states of Al^{11+} for different Debye Screening Parameters

	-E (in a.u.)							
D	$2p^2$	2p3p	2p4p	2p5p	2p6p	2p7p	2p8p	$Al^{12+}(2p)$
∞	40.156 443	29.297 506	25.700 869	24.044 136	23.147 689	22.608 682	22.259 576	21.125 000
50	39.658 380	28.800 920	25.206 317	23.552 172	22.658 838	22.123 440	21.778 408	20.865 997
20	38.918 498	28.068 647	24.484 342	22.843 004	21.964 675	21.446 171	21.119 616	20.481 203
10	37.704 307	26.880 829	23.331 234	21.731 664	20.900 523	20.433 131	20.160 260	19.849 629
5	35.345 189	24.621 741	21.197 969	19.742 393	19.065 459	18.755 773	18.638 042	18.622 129
4	34.199 343	23.547 629	20.210 904	18.851 144	18.272 519	18.058 276		18.025 733
3	32.338 096	21.835 335	18.674 059	17.501 331	17.107 408			17.056 707
2	28.791 278	18.685 943	15.247 773					15.209 105

Enlarged view of the stabilization diagram (given in figure 1) for $^3P^e$ state of Al^{11+} in the energy range -20 a.u. to -10 a.u. is given in figure 3. The $^3P^e$ state of Al^{11+} below N=3 ionization threshold of Al^{12+} can arise due to 3*pnp* and 3*dmd* (n, $m \geq 3$) configurations. It is worthwhile to mention that Ho and Bhatia [24] and Saha and Mukherjee [66] quoted that the odd number of states *i.e.* $^3P^e$ (1), $^3P^e$ (3), $^3P^e$ (5)… *etc* below N = 3 hydrogenic threshold are due to 3*pnp* configuration whereas the even number of states *i.e.* $^3P^e$ (2), $^3P^e$ (4), $^3P^e$ (6)… *etc* are due to 3*dmd* configuration. It is clear from figure-3 that consecutive two states due to 3*pnp* and 3*dmd* configurations (n, $m \geq 3$) with $n = m$ *i.e.* $3p^2$ and $3d^2$, *3p4p* and *3d4d*… *etc*. are appearing as a 'pair' of $^3P^e$ states. Such type of paring was also evident from

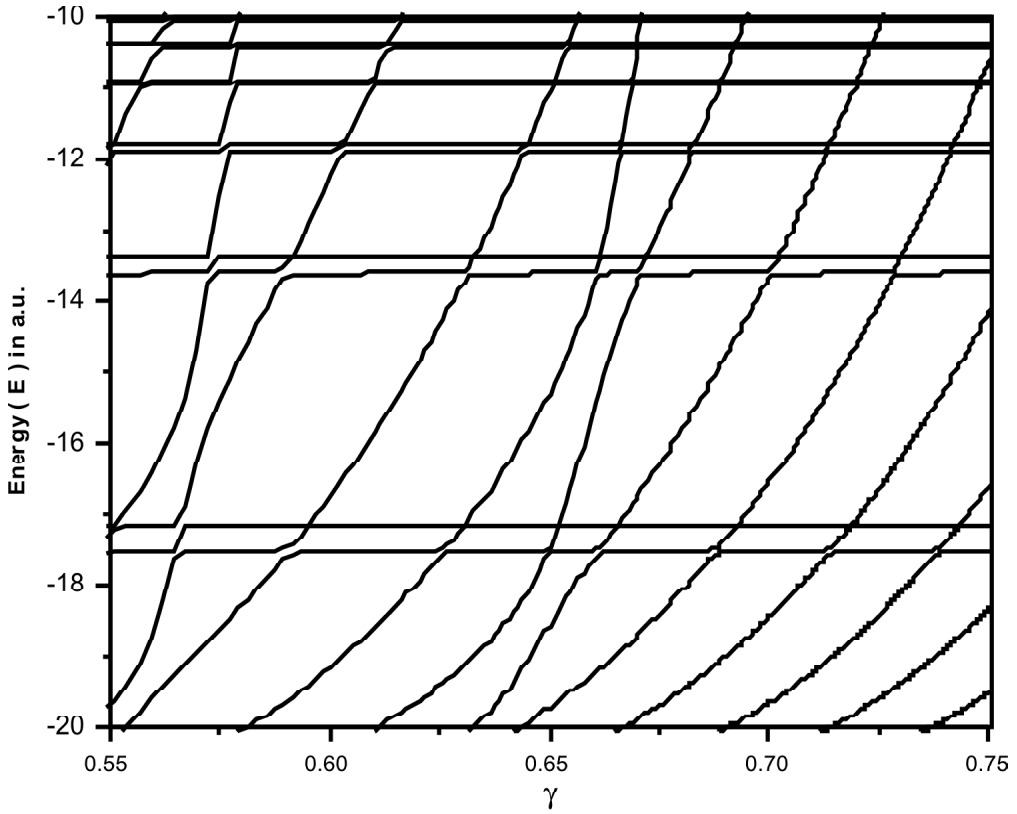

Figure 3: Enlarged view of the stabilization diagram for $^3P^e$ states of Al^{11+} below N=3 ionization threshold of Al^{12+} in Debye plasma of D= 50 a.u. in the energy range -20 a.u. to -10 a.u.

the calculations of resonance parameters of $^3P^e$ states of helium below N = 3 ionization threshold of He^+ due to Saha and Mukherjee [66] as well from the estimation of resonance parameters of $^1S^e$ states of two-electron atoms (Z=3-8) below N = 2 hydrogenic threshold due to Saha *et al.* [28]. From a closer look at figure 3, we can see that for a short range of γ each eigenroot between N = 2 and N = 3 ionization thresholds of Al^{12+} becomes almost flat in the vicinity of avoided crossings in the neighborhood of a particular resonance state. The density of states ρ(E) is calculated by evaluating the inverse of the slope at a number of points near the flat plateau of each energy eigenroot using the formula [66, 67] given by:

$$\rho_n(E) = \left| \frac{\gamma_{i+1} - \gamma_{i-1}}{E_n(\gamma_{i+1}) - E_n(\gamma_{i-1})} \right|_{E_n(\gamma_i)=E_i} \tag{6}$$

The calculated density of resonance states $\rho_n(E)$ is then fitted to the following Lorentzian form [66, 67]:

$$\rho_n(E) = y_0 + \frac{A}{\pi} \frac{\Gamma/2}{(E - E_r)^2 + (\Gamma/2)^2} \tag{7}$$

where, y_0 is the baseline background, A is the total area under the curve from the baseline, E_r gives the position of the centre of the peak of the curve and Γ represents the full width of the peak of the curve at half height. Among different fitting curves for each eigenroot corresponding to a particular resonance state, the fitting curve with least χ^2 and the square of correlation closer to unity leads to the desired resonance energy (E_r) and width (Γ) as mentioned in ref. [66]. The evaluation of density of states following the fitting procedure is being repeated for each value of the Debye screening parameter (μ). For example, the calculated density and the corresponding fitted Lorentzian for the $3d^2$ ($^3P^e$) resonance state of Al^{11+} below Al^{12+} (3s) for Debye length D = 50 a.u. is given in figure 4 which yields resonance position E_r at -17.12642 a.u. and width Γ = 7.88 (10^{-5}) a.u.

A similar stabilization diagram for $^3P^e$ state of Al^{11+} embedded in plasma of Debye length D = 3 a.u. is displayed in Figure 5. It is to be noted from figure 5 that the number of bound 2pnp ($^3P^e$) states below Al^{12+} (2p) and the number of $^3P^e$ resonance states below Al^{12+} (3s) are lesser than the number of those states of plasma embedded Al^{11+} for D = 50 a.u. as given in figure 1. The calculated density and the corresponding fitted Lorentzian for the $3p^2$ ($^3P^e$) resonance state of Al^{11+} below Al^{12+} (3s) for Debye length D = 3 a.u. is given in figure 6 which yields resonance position E_r at –10.85699 a.u. and width Γ = 0.00057071 a.u. The calculated resonance parameters of $^3P^e$ states due to 3pnp [n = 3-8] and those due to 3dmd [m = 3-7] configuration of Al^{11+} along with Al^{12+} (3s) energies are given in table 2 and table 3 respectively. To see the variation of resonance parameters with increasing plasma strength, we have plotted the resonance energies of 3pnp [n=3-8] $^3P^e$ states as a function of Debye parameter (μ) and Debye length (D) in figure 7(a) and 7(b) respectively while the resonance energies of 3dnd [n=3-7] $^3P^e$ states are displayed as a function of Debye parameter (μ) and Debye length (D) in figure 8(a) and 8(b) respectively. Gradual approach of all the $^3P^e$ resonance states toward the continuum (figure 7 and figure 8) with the increase in plasma screening parameter suggests that the system becomes less and less stable as we move towards stronger screening region. Similarly we have plotted the autoionization width of 3pnp [n=3-8] $^3P^e$ states as a function of Debye parameter (μ) and Debye length (D) in figure 9(a) and 9(b) respectively while the width of 3dnd [n=3-7] $^3P^e$ states are displayed as a function of Debye parameter (μ) and Debye length (D) in figure 10(a) and 10(b) respectively. It is evident from figure 9 and figure 10 that the width of 3pnp [n=3-8] $^3P^e$ resonance state gradually decreases with increase in Debye parameter (μ) while the width of 3dmd [m=3-7] $^3P^e$ resonance state increases monotonically with increase in Debye parameter (μ). Such type of variation of width of 3pnp [n=3-6] and 3dmd [m=3-5] $^3P^e$ states of plasma embedded helium was noted earlier by Kar and Ho [68]. Thus it is remarkable to note that the width of the resonance states of a particular symmetry arising from different configurations behaves differently with the variation of plasma screening parameter.

Table 2

Resonance Energies $-E_r$ (in a.u.) and widths Γ (in a.u.) of doubly excited 3pnp [n = 3-8] $^3P^e$ resonance states of Al^{11+} below N = 3 ionization threshold of Al^{12+} for various Debye screening parameters (μ). The uncertainty of the resonance positions and widths is given in the parenthesis

	3p3p		*3p4p*		*3p5p*		*3p6p*		*3p7p*		*3p8p*		Al^{12+}*(3s)*
D	$-E_r$	Γ	$-E_r$	Γ	$-E_r$	Γ	$-E$	Γ	$-E_r$	Γ	$-E_r$	Γ	$-E$
∞	**18.00543**	**0.0065092**	**14.10424**	**0.0038508**	**12.38426**	**0.00177 36**	**11.45667**	**9.5113E-4**	**10.90137**	**5.6204E-4**	**10.54311**	**3.4929E-4**	9.388888
	[6.2074E-7]	[2.3288E-6]	[7.6578E-7]	[3.1985E-6]	[3.2855E-7]	[1.4106E-6]	[2.4105E-7]	[1.1009E-6]	[1.4452E-7]	[7.3522E-7]	[4.2261E-8]	[2.2238E-7]	
50	**17.5101**	**0.0065029**	**13.61089**	**0.0038477**	**11.89342**	**0.0017697**	**10.9689**	**9.4673E-4**	**10.41715**	**5.5715E-4**	**10.06292**	**3.4538E-4**	9.131567
	[1.1087E-6]	[4.5158E-6]	[7.7146E-7]	[3.3475E-6]	[3.2852E-7]	[1.4561E-6]	[2.447E-7]	[1.1848E-6]	[1.4538E-7]	[7.6874E-7]	[5.1402E-8]	[2.5432E-7]	
20	**16.78428**	**0.0064875**	**12.89515**	**0.0038270**	**11.19016**	**0.0017480**	**10.28045**	**9.2363E-4**	**9.745470**	**5.3423E-4**	**9.40958**	**3.2492E-4**	8.755443
	[1.5808E-6]	[7.417E-6]	[7.6311E-7]	[3.5073E-6]	[3.2872E-7]	[1.573E-6]	[2.3521E-7]	[1.0918E-6]	[1.3559E-7]	[6.4389E-7]	[8.0362E-8]	[3.9535E-7]	
10	**15.61892**	**0.0064251**	**11.76402**	**0.0037486**	**10.10005**	**0.0016710**	**9.23732**	**8.4647E-4**	**8.75353**	**4.5717E-4**	**8.47157**	**2.5092E-4**	8.153905
	[1.1072E-6]	[4.582E-6]	[7.5303E-7]	[3.6061E-6]	[3.1352E-7]	[1.4711E-6]	[2.1731E-7]	[1.0229E-6]	[1.1716E-7]	[5.6222E-7]	[7.9334E-8]	[4.5408E-7]	
5	**13.4466**	**0.0061923**	**9.71726**	**0.0034558**	**8.19678**	**0.0013941**	**7.48978**	**5.8837E-4**	**7.16579**	**2.2764E-4**			7.040164
	[1.071E-6]	[4.4361E-6]	[7.3155E-7]	[4.2948E-6]	[3.7111E-7]	[1.7511E-6]	[1.5913E-7]	[8.5113E-7]	[4.5785E-8]	[2.2353E-7]			
4	**12.43579**	**0.0060406**	**8.79421**	**0.0032516**	**7.37021**	**0.0012189**	**6.76307**	**4.4346E-4**	**6.66049**	**9.3886E-5**			6.525185
	[1.0005E-6]	[5.3712E-6]	[6.7376E-7]	**[3.4182E-6]**	[2.3532E-7]	[1.1278E-6]	[1.1633E-7]	[5.6152E-7]	[7.4442E-9]	[3.5387E-8]			
3	**10.85699**	**0.0057071**	**7.39353**	**0.0028664**	**6.15867**	**9.136E-4**	**5.73913**	**2.2663E-4**					5.724792
	[9.6711E-7]	[5.2587E-6]	[5.9704E-7]	[2.9536E-6]	[1.8081E-7]	[8.8534E-7]	[1.8073E-7]	[8.4621E-7]					
2	**8.07194**	**0.0049123**	**5.06418**	**0.0020350**	**4.28499**	**3.5264E-4**							4.324302
	[8.572E-7]	[4.5202E-6]	[4.3811E-7]	[2.1695E-6]	[3.2155E-7]	[1.6422E-6]							

Table 3
Resonance energies $-E_r$ (in a.u.) and widths Γ (in a.u.) of doubly excited $3pnp$ [n = 3-8] $^3P^e$ resonance states of Al^{11+} below N = 3 ionization threshold of Al^{12+} for various Debye screening parameters (μ). The uncertainty of the resonance positions and widths is given in the parenthesis

	3d3d		*3d4d*		*3d5d*		*3d6d*		*3d7d*		$Al^{12+}(3s)$
	$-E_r$	Γ	$-E_r$	Γ	$-E_r$	Γ	$-E_r$	Γ	$-E_r$	Γ	$-E$
∞	**17.6222** [1.1175E-8]	**7.781E-5** [5.4917E-8]	**13.89145** [6.4802E-9]	**3.2455E-5** [3.1331E-8]	**12.27398** [2.2303E-9]	**8.7471E-6** [1.0268E-8]	**11.39272** [6.71E-10]	**2.9999E-6** [3.1287E-9]	**10.86114** [4.0043E-9]	**1.2187E-6** [1.894E-8]	9.388 888
50	**17.12642** [1.1327E-8]	**7.88E-5** [5.5755E-8]	**13.39779** [6.6256E-9]	**3.343E-5** [3.1357E-8]	**11.78295** [2.4164E-9]	**9.4712E-6** [1.1125E-8]	**10.90484** [8.1853E-10]	**3.5666E-6** [3.8129E-9]	**10.37689** [3.8026E-9]	**1.7118E-6** [1.8046E-8]	9.131 567
20	**16.39833** [1.1969E-8]	**8.3904E-5** [5.6248E-8]	**12.68045** [7.5780E-9]	**3.8533E-5** [3.5206E-8]	**11.07866** [3.4709E-9]	**1.3445E-5** [1.6302E-8]	**10.21574** [1.7045E-9]	**6.9701E-6** [7.9359E-9]	**9.70481** [5.6168E-9]	**4.6562E-6** [2.6131E-8]	8.755 443
10	**15.22508** [1.4797E-8]	**1.0194E-4** [7.066E-8]	**11.54358** [1.1301E-8]	**5.7312E-5** [5.2711E-8]	**9.98437** [7.7743E-9]	**2.9902E-5** [3.6469E-8]	**9.16925** [5.9393E-9]	**2.2986E-5** [2.8066E-8]	**8.70985** [5.9908E-9]	**2.0531E-5** [2.768E-8]	8.153 905
5	**13.02162** [2.6214E-8]	**1.7285E-4** [1.2827E-7]	**9.47266** [2.6866E-8]	**1.3491E-4** [1.2652E-7]	**8.06049** [2.6352E-8]	**9.9789E-5** [1.2554E-7]	**7.40226** [2.0249E-8]	**7.9001E-5** [9.5744E-8]	**7.10366** [1.0652E-7]	**5.9343E-5** [5.0207E-7]	7.040 164
4	**11.98756** [3.4314E-8]	**2.2304E-4** [1.6846E-7]	**8.5308** [3.7303E-8]	**1.8731E-4** [1.7303E-7]	**7.21709** [3.5982E-8]	**1.3717E-4** [1.6675E-7]	**6.53598** [1.1777E-6]	**9.5612E-5** [5.8641E-6]			6.525 185
3	**10.35889** [5.0203E-8]	**3.1753E-4** [2.513E-7]	**7.08962** [5.5551E-8]	**2.7179E-4** [2.6953E-7]	**5.97092** [3.2762E-8]	**1.726E-4** [1.51E-7]					5.724 792
2	**7.43796** [8.0184E-8]	**4.8269E-4** [4.232E-7]	**4.65795** [7.4855E-8]	**3.516E-4** [3.7786E-7]							4.324 302

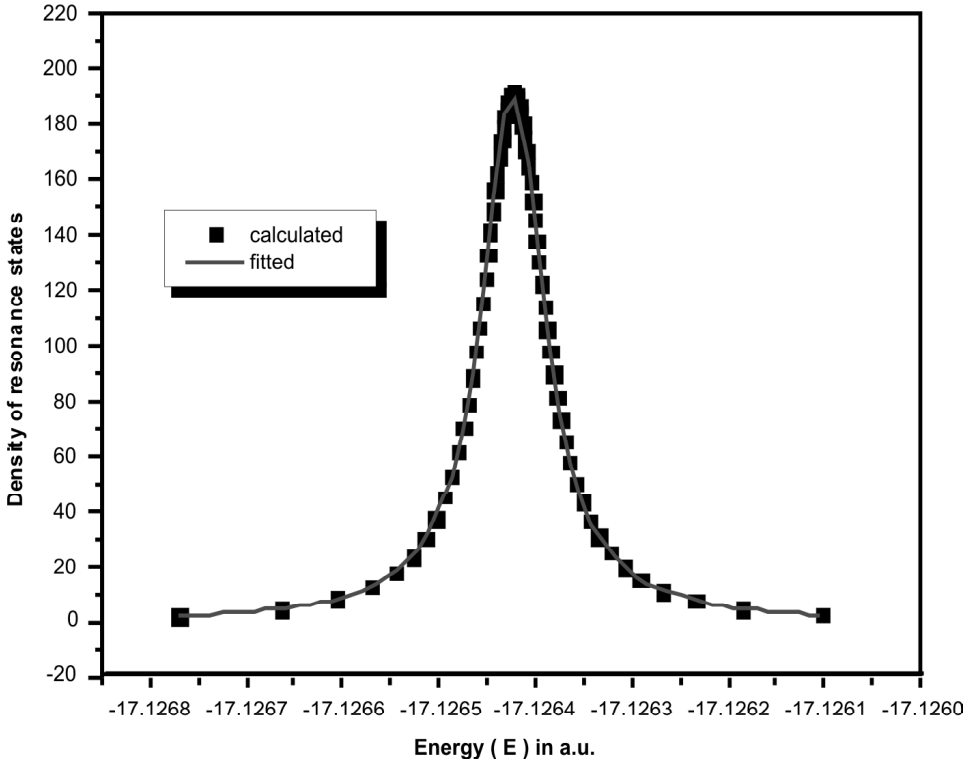

Figure 4: Calculated density (squares) and the fitted Lorentzian (solid line in red) for the $3d^2$ ($^3P^e$) resonance state [E_r= -17.12642 a.u. and Γ = 7.88 (-5) a.u.] of Al^{11+} under Debye plasma of D = 50 a.u.

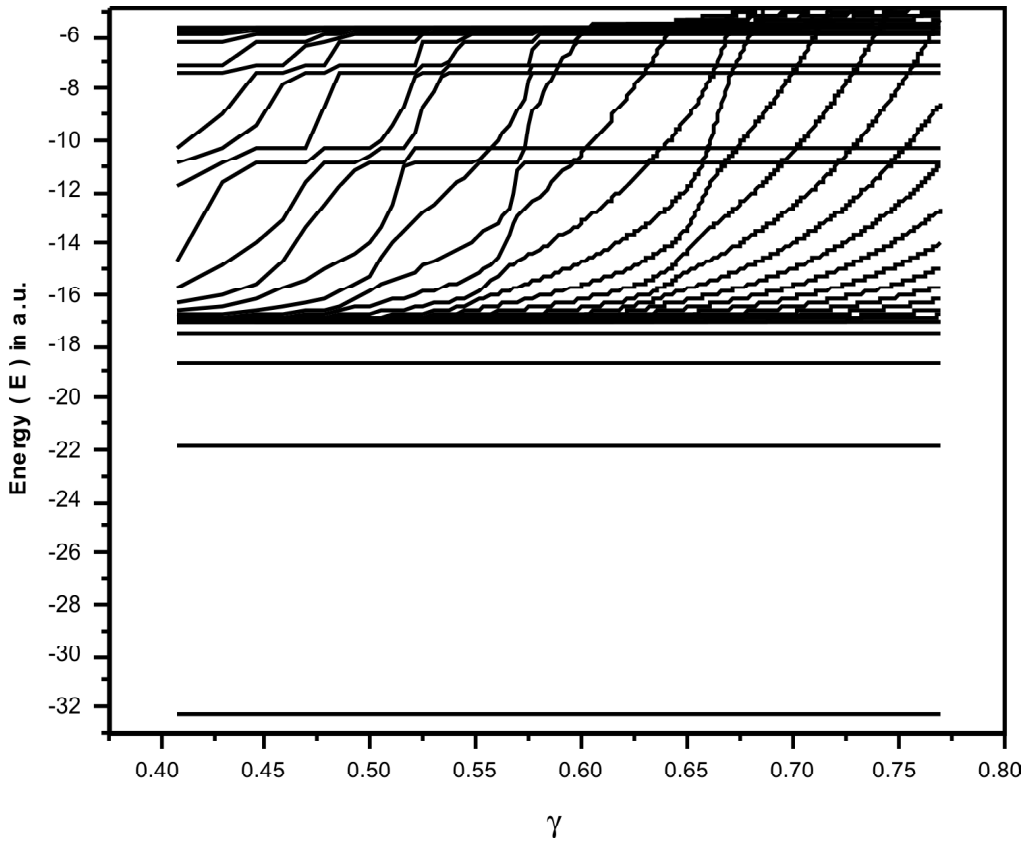

Figure 5: Stabilization diagram for $^3P^e$ states of Al^{11+} in Debye plasma of D = 3 a.u.

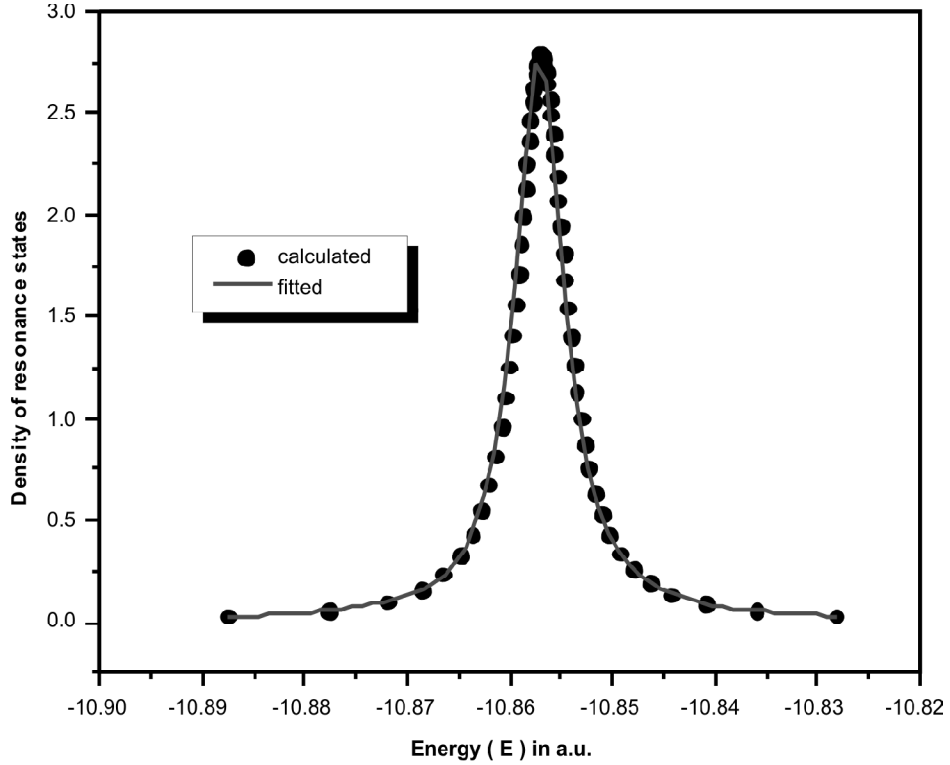

Figure 6: Calculated density (squares) and the fitted Lorentzian (solid line in red) for the $3p^2$ ($^3P^e$) resonance state [E_r = –10.85699 a.u. and Γ = 0.0057071 a.u.] of Al^{11+} under Debye plasma of D = 3 a.u.

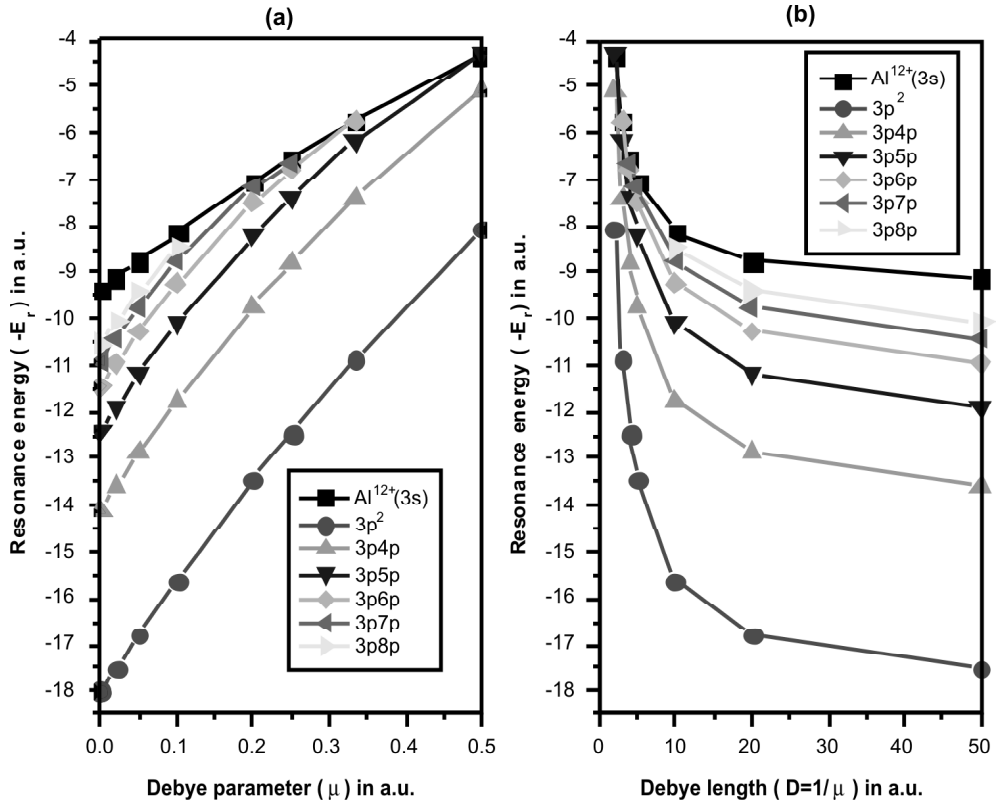

Figure 7: The variation of the resonance $3pnp$ (n=3-8) ($^3P^e$) state energies of Al^{11+} along with Al^{12+} (3s) energies vs. different Debye screening parameter (μ) is given in (a) and that with Debye length (D) is given in (b)

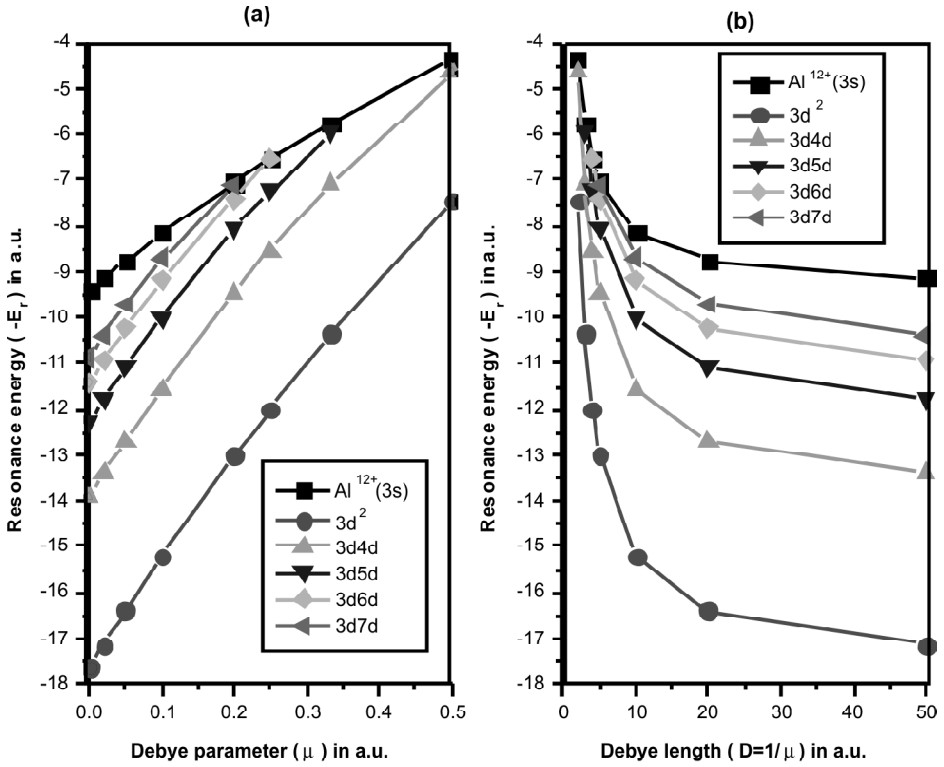

Figure 8: The variation of the resonance 3*dnd* (*n*=3-7) ($^3P^e$) state energies of Al^{11+} along with Al^{12+} (3s) energies vs. different Debye screening parameter (μ) is given in (a) and that with Debye length (*D*) is given in (b)

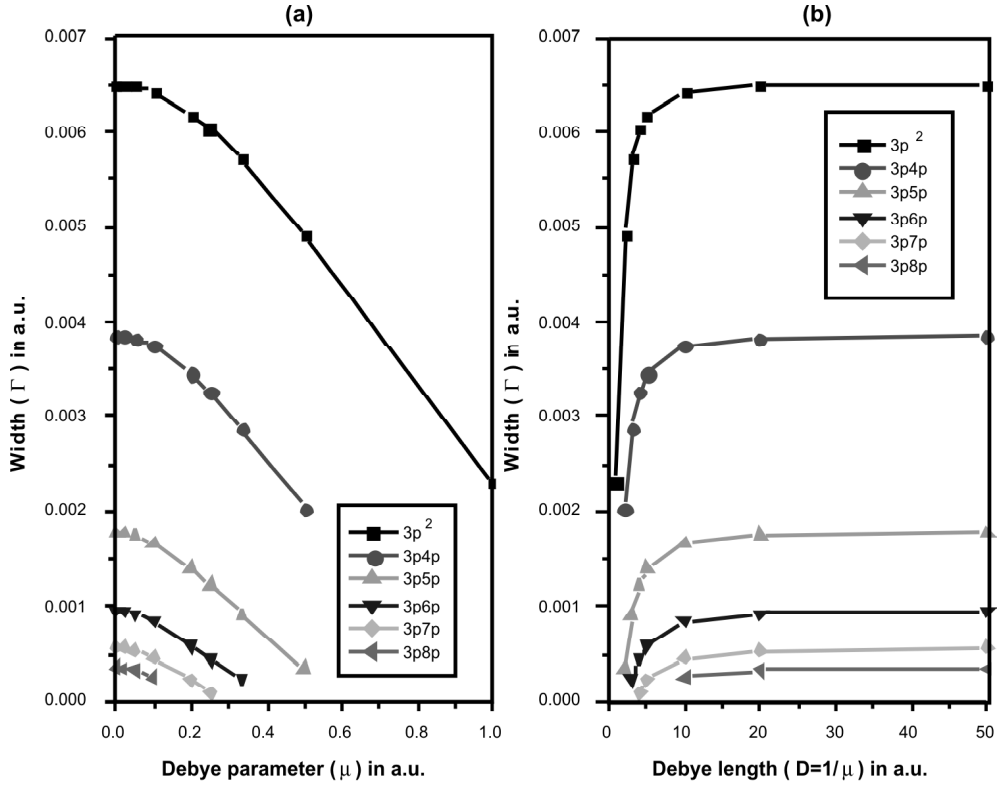

Figure 9: The variation of width of the resonance 3*pnp* (*n*=3-8) ($^3P^e$) states of Al^{11+} vs. different Debye screening parameter (μ) is given in (a) and that with Debye length (*D*) is given in (b)

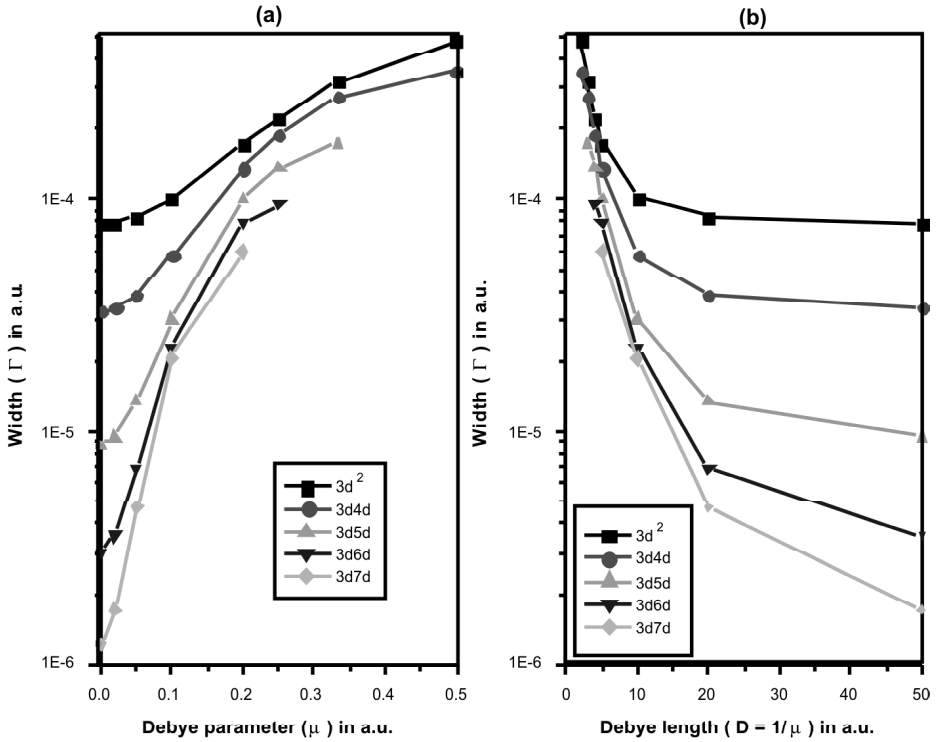

Figure 10: The variation of width of the resonance 3*dnd* (*n* = 3-7) ($^3P^e$) states of Al^{11+} vs. different Debye screening parameter (μ) is given in (a) and that with Debye length (*D*) is given in (b)

IV. CONCLUSION

Metastable bound and resonance states of highly stripped atoms embedded in weakly coupled plasma can be studied effectively by using Ritz-variational method and Stabilization method respectively with explicitly correlated Hylleraas basis sets. Our calculations on the energy levels of plasma embedded helium-like aluminum yields very consistent and accurate atomic data. It is evident that the overall behavior of resonance parameters of all $^3P^e$ states as a function of plasma screening follows similar patterns for all the excited states which establish the general consistency of the reported values. The methodology employed in the present work can be extended to study the effect of plasma on other two electron atoms for which relativistic correction is not so high. We hope that our findings will help the future workers in the field of atomic physics, plasma physics and astrophysical data analysis.

Acknowledgements

Authors are thankful to the Department of Atomic Energy, BRNS, Government of India, for the financial assistance under Grant number 2011/37P/15/BRNS/0074. SB is thankful to USIEF for the Fulbright-Nehru fellowship (2012-2013) for the stay at Auburn, USA. Authors are grateful to Prof. E. Oks for providing some useful references.

References

[1] V. Kharchenko, A. Bhardwaj, A. Dalgarno, D. R. Schulz, P. C. Stancil, *J. Geophys. Res.* **113,** A08229, (2008).

[2] A.B.C. Walker Jr., H. R. Rugge, *Astrophys. J.* **164,** 181, (1971).

[3] A. H. Gabriel, C. Jordan, *Nature* **221,** 94, (1969).

[4] T. Fujimoto, T. Kato, *Astrophys. J.* **246,** 994, (1981).

[5] R. P. Madden, K. Codling, *Phys. Rev. Lett.* **10,** 516, (1963).

[6] J. L. Tech, J. F. Ward, *Phys. Rev. Lett.* **27,** 367, (1971).

[7] J. P. Buchet, M. C. Buchet-Poulizac, H. G. Berry, G. W. F. Drake, *Phys. Rev. A* **7,** 922, (1973).

[8] P. J. Hicks, J. Comer, *J. Phys. B At. Mol. Opt. Phys.* **8,** 1866, (1975).

[9] M. Rodbro, R. Bruch, P. Bisgaard, *J. Phys. B: Atom. Mol. Phys.* **12,** 2413, (1979).

[10] H. A. Sakaue *et al.*, *J. Phys. B: Atom. Mol. Opt. Phys.* **23,** L401, (1990).

[11] Y. Kanai, H. A. Sakaue, S. Ohtani, K. Wakiya, H. Suzuki, T. Takayanagi, T. Kambara, A. Danjo, M. Yoshino and Y. Awaya, Z. Phys. D: *Atom. Mol. Clus.* **21,** S225, (1991).

[12] M. Domke, G. Remmers, G. Kaindl, *Phys. Rev. Lett.* **69,** 1171, (1992).

[13] K. Schulz, G. Kaindl, M. Domke, J. D. Bozek, P. A. Heimann, A. S. Schlachter and J. M. Rost, *Phys. Rev. Lett.* **77,** 3086, (1996).

[14] M. K. Odling-Smee, E. Sokell, P. Hammond, M.A. MacDonald, *Phys. Rev. Lett.* **84,** 2598, (2000).

[15] T. W. Gorczyca, J. E. Rubensson, C. Såthe, M. Ström, M. Agåker, D. Ding, S. Stranges, R. Richter and M. Alagia, *Phys. Rev. Lett.* **85,** 1202, (2000).

[16] F. Penent, P. Lablanquie, R. I. Hall, M. Žitnik, K. Bucar, S. Stranges, R. Richter, M. Alagia, P. Hammond and J. G. Lambourne, *Phys. Rev. Lett.* **86,** 2758, (2001).

[17] J. G. Lambourne, F. Penent, P. Lablanquie, R. I. Hall, M. Ahmad, M. Žitnik, K. Bucar, M. K. Odling-Smee, J. R. Harries, P. Hammond, D. K. Waterhouse, S. Stranges, R. Richter, M. Alagia, M. Coreno and M. Ferianis, *Phys. Rev. Lett.* **90,** 153004, (2003).

[18] J. Cooper, U. Fano, F. Prats, *Phys. Rev. Lett.* **10,** 518, (1963).

[19] G.W.F. Drake, A. Dalgarno, *Phys. Rev. A* **1,** 1325, (1970).

[20] A. K. Bhatia, *Phys. Rev. A* **9,** 9, (1974).

[21] D. R. Herrick, *Adv. Chem. Phys.* **52,** 1, (1983).

[22] U. Fano, *Rep. Prog. Phys.* **46,** 97, (1983).

[23] C. D. Lin, *Adv. At. Mol. Phys.* **22,** 77, (1986).

[24] Y. K. Ho and A. K. Bhatia, *Phys. Rev. A* **47,** 2628, (1993).

[25] T. K. Mukherjee, P. K. Mukherjee, *Phys. Rev. A* **69,** 064501, (2004).

[26] S. Bhattacharyya, J. K. Saha, T. K. Mukherjee, and P. K. Mukherjee, *Phys. Rev. A* **78,** 032505, (2008) and references therein.

[27] J. K. Saha, S. Bhattacharyya, T. K. Mukherjee and P. K. Mukherjee, *Chem. Phys. Lett.* **478,** 292, and (2009) references therein.

[28] J. K. Saha, S. Bhattacharyya, T. K. Mukherjee, P. K. Mukherjee, *Int. J. Quant. Chem.* **111,** 1819, (2011).

[29] J. Eiglsperger, B. Piraux and J. Madronero, *Phys. Rev. A* **81,** 042527, (2010).

[30] Z. Jiang, S. Kar and Y K Ho *Phys. Scr.* **85,** 065304, (2012) and references therein.

[31] S. Nakazaki, K. Sakimoto, Y. Itikawa, *Phys. Scr.* **47,** 359, (1993).

[32] W. Schwanda, K. Eidman, *Phys. Rev. Lett.* **69,** 3507, (1992).

[33] St. Boddeker, S. Gunter, A. Konies, L. Hitzschke, H. J. Kunze, *Phys. Rev. E* **47,** 2785, (1990).

[34] A. B. C. Walker Jr., H. R. Rugge, *Astrophys. J.* **164,** 181, (1971).

[35] G. A. Doschek, P. Meekins, R.W. Kerplin, T.A. Chubb, H. Friedman, *Astrophys. J.* **164,** 165, (1971).

[36] J. L. Culhane *et. al.*, *Sol. Phys.* **136,** 89, (1991).

[37] U. Feldman, *Phys. Scr.* **46**, 202, (1992).

[38] RESIK & Diogeness NEWS, Week 42, (2002).

website : http://www.cbk.pan.wroc.pl/resik_archive/resik_weekly_14-20_Oct/News.htm

[39] J. Sylwester, B Sylwester, K. J. H. Phillips, *Astrophys. J.* **681,** L117, (2008).

[40] C. Chang and W. Cui, *Astrophys. J.* **663**, 1207, (2007).

[41] S. Kaspi *et al., Astrophys. J.* **574**, 643, (2002).

[42] T. Holczer, E. Behar and N. Arav, *Astrophys. J.* **708**, 981, (2010).

[43] S. Watanabe, M. Sako, M. Ishida, Y. Ishisaki, S. M. Kahn, T. Kohmura, F. Nagase, F. Paerels and T. Takahashi, *Astrophys. J.* **651**, 421, (2006).

[44] R. Nordon and E. Behar, *Astronomy & Astrophysics* **464**, 309, (2007).

[45] M. Hanke, J. Wilms, M. A. Nowak, K. Pottschmidt, N. S. Schulz and J. C. Lee, *Astrophys. J.* **690**, 330, (2009).

[46] J. R. Peterson, S. M. Kahn, F. B. S. Paerels, J. S. Kaastra, T. Tamura, J. A. M. Bleeker, C. Ferrigno and J. G. Jernigan, *Astrophys. J.* **590**, 207, (2003).

[47] M. Loewenstein and D. S. Davis, *BAAS*, **41**, 483, (2010).

[48] T. R. Kallman, M. A. Bautista, S. Goriely, C. Mendoza, J. M. Miller, P. Palmeri, P. Quinet and J. Raymond, *Astrophys. J.* **701**, 865, (2009).

[49] N. S. Schulz, D. P. Huenemoerder, L. Ji, M. Nowak, Y. Yao and C. R. Canizares, *Astrophys. J.* **692**, L80, (2009).

[50] D. P. Huenemoerder, C. R. Canizares, J. J. Drake and J. Sanz-Forcada, *Astrophys. J.* **595**, 1131, (2003).

[51] I. N. Kosarev, C. Stehlé, N. Feautrier, A. V. Demura and V. S. Lisitsa, *J. Phys. B: At. Mol. Opt. Phys.* **30,** 215, (1997).

[52] P. Palmeri, P. Quinet, C. Mendoza, M. A. Bautista, J. García, M. C. Witthoeft and T. R. Kallman, *Astronomy & Astrophysics* **525**, A59, (2011).

[53] P. Sauvan, E. Dalimier, E. Oks, O. Renner, S. Weber and C. Riconda, *Int. Review of Atomic and Molecular Phys.* **1**, 123, (2010).

[54] O. Renner, P. Sauvan, E. Dalimier, C. Riconda, F. B. Rosmej, S. Weber, P. Nicolai, O. Peyrusse, I. Uschmann, S. Höfer, R. Loetzsch, E. Förster, E. Oks, High Energy Density Physics, **5**, 139, (2009).

[55] E. Dalimier, E. Oks, O. Renner and R. Schott, *J. Phys. B: Atom. Mol. Phys.* **40**, 909, (2007).

[56] O. Renner, E. Dalimier, E. Oks, F. Krasniqi, E. Dufour, R. Schott and E. Förster, *J. Quant. Spectr. Rad. Transfer*, **99**, 439, (2006).

[57] E. Leboucher-Dalimier, E. Oks, E. Dufour, P. Sauvan, P. Angelo, R. Schott and A. Poquerusse, *Phys. Rev. E, Rapid Comm.* **64**, 065401, (2001).

[58] A.N. Sil, P.K. Mukherjee, *Int. J. Quant. Chem.* **102**, 1061, (2005).

[59] S. Kar and Y. K. Ho, *J. Phys. B* **42**, 044007, (2009).

[60] A. I. Akhiezer, I. A. Akhiezer, R. A. Polovin, A. G. Sitenko and K. N. Stepanov, *Plasma Electrodynamics, Vol. 1. Linear Response Theory* (Oxford: Pergamon) (1975).

[61] V. A. Mandelshtam, T. R. Ravuri and H. S. Taylor, *Phys. Rev. Lett.* **70**, 1932, (1993).

[62] T. K. Mukherjee and P. K. Mukherjee, *Phys. Rev. A* **50**, 850, (1994).

[63] J. K. Saha, S. Bhattacharyya, T. K. Mukherjee, P. K. Mukherjee, *J. Phys. B: Atom. Mol. Phys* **42**, 245701, (2009).

[64] J. A. Nelder and R. Mead, *Comput. J.* **7**, 308, (1965).

[65] J. K. Saha, S. Bhattacharyya and T. K. Mukherjee, *J. Chem Phys.* **132**, 134107, (2010).

[66] J. K. Saha and T. K.Mukherjee, *Phys. Rev. A* **80**, 022513, (2009).

[67] S. S. Tan and Y. K. Ho, *Chin. J. Phys.* **35**, 701, (1997).

[68] S. Kar and Y.K.Ho, *J. Phys. B: Atom. Mol. Phys* **40**, 1403, (2007).